Supplementary Information

Materials and Methods

BS–AuNP solution preparation. Citrate-covered standard AuNPs of 20 nm in average diameter are prepared following the previous study (36). Briefly, gold chloride (III) trihydrate ($HAuCl_4 \cdot 3H_2O$) is dissolved in deionized Milli-Q water (1.0×10^{-3} mol/L) under refluxing. Sodium citrate tribasic dihydrate solution in deionized water (4×10^{-2} mol/L) is added to the solution. Reaction-completion is detected by a color change from pale yellow to wine red. The AuNP solution is dialyzed overnight using a Spectra/Por®7 membrane (1,000 Da cut) against deionized Milli-Q water to remove excess sodium citrate tribasic dihydrate. The concentration of the AuNP solution is fixed to 1.2×10^{19} AuNPs/m^3 in consideration of the 20 nm diameter (denoted as AuNP standard stock solution in this study). Considering the volume of an Au atom (v_{Au} = 17 Å^3), the number of Au atoms in a spherical particle of 10 nm radius (r) is approximately a quarter of a million based on the relation $N_{Au} = 4\pi r^3/3v_{Au}$. On the basis of the Au concentration ($HAuCl_4$, 2.5×10^{-4} mol/L), the average number density of AuNPs in a solution is around 1×10^{-9} mmol AuNP/mL. 1,3,4-Thiadiazole-2,5-dithiol (Bismuthiol I, $C_2H_2N_2S_3$, M_W = 150.25, denoted as BS in this study) is dissolved in ethanol (1×10^{-4} mmole BS/mL, BS standard stock solution). The peak absorbance wavelength of BS in UV-vis spectrum is around 320 nm (37). To the AuNP standard stock solution 100 mL, 0.1 ($N_{BS}/N_{AuNP} = 0.1 \times 10^3$), 0.2 ($N_{BS}/N_{AuNP} = 0.2 \times 10^3$), 0.3 ($N_{BS}/N_{AuNP} = 0.3 \times 10^3$), 0.5 ($N_{BS}/N_{AuNP} = 0.5 \times 10^3$), 1 ($N_{BS}/N_{AuNP} = 1 \times 10^3$), 1.2 ($N_{BS}/N_{AuNP} = 1.5 \times 10^3$), 1.5 ($N_{BS}/N_{AuNP} = 0.5 \times 10^3$), 1.8 ($N_{BS}/N_{AuNP} = 1.8 \times 10^3$), 2 ($N_{BS}/N_{AuNP} = 2 \times 10^3$), 2.5 ($N_{BS}/N_{AuNP} = 2.5 \times 10^3$), 3 ($N_{BS}/N_{AuNP} = 3 \times 10^3$) and 4 ($N_{BS}/N_{AuNP} = 4 \times 10^3$) mL of BS standard stock solution is added and reacted for 24 hrs at room temperature (Table 1). The solutions are dialyzed overnight using a Spectra/Por®7 membrane (1,000 Da cut) against ethanol to remove excess 1,3,4-thiadiazole-2,5-dithiol and check for residual free BS in the dialysis ethanol solution by UV-vis spectroscopy to confirm the reaction completion. The solutions are finally dialyzed by DI water to exchange the dispersing media.

BS-linked AuNP network formation. Dithiol-functionalized Bismuthiol (BS) is expected to link AuNPs according to the ratio [number of BS, N_{BS}]/[number of AuNP, N_{AuNP}] suggested in Fig. 1a. The following assumptions are used to set up the conditions,

1. There is no free BS in the solution (UV-vis spectroscopy experimentally confirms that there is no detectable free BS in the sample)
2. All the AuNPs have the same number of BS on each surface and they are identical in size and functionality under the given condition
3. Dithiol groups of a single BS do not attach on the same AuNP

To investigate the number of BS–AuNP cluster in the given system, following relation is suggested,

$$N_{AuNP} \times \boldsymbol{A} \times \boldsymbol{P} = N_{BS} \times \boldsymbol{B} \times \boldsymbol{I} + N_{BS} \times \boldsymbol{B} \times (1 - \boldsymbol{I}) \quad \text{(S1)}$$

N_{AuNP}: total # of AuNPs

N_{BS}: total # of BS

$\boldsymbol{A}$: # of functional site of a single AuNP on which BS can attach

$\boldsymbol{B}$: # of functional site on a single BS (which is 1 or 2)

$\boldsymbol{P}$: degree of BS reaction on a single AuNP = [reacted $\boldsymbol{A}$]/[total $\boldsymbol{A}$], $0 \leq \boldsymbol{P} \leq 1$

$\boldsymbol{I}$: fraction of one-end free BS (having dangling end) = [one-end free BS]/[total BS], $0 \leq \boldsymbol{I} \leq 1$

Two extreme cases **I** and **III** can be considered as follows,

Case I. $\boldsymbol{I} = 1$, B = 1,

$$\boldsymbol{A} \times \boldsymbol{P} = N_{BS}/N_{AuNP} \qquad [0 \leq \boldsymbol{P} \leq 1] \quad \text{(S2)}$$

Since all BS are one-end active, the number of BS–AuNP clusters is the same as the number of the given AuNPs. The ratio N_{BS}/N_{AuNP} decides the number of BS on a single AuNP. The corresponding schematic is illustrated in Fig. 1A (ii to iv).

Case III. $\boldsymbol{I} = 0$, B = 2,

$$\boldsymbol{A} \times \boldsymbol{P} = 2N_{BS}/N_{AuNP} \qquad [0 \leq \boldsymbol{P} \leq 1] \quad \text{(S3)}$$

Since all BS are dual-end active, all the BS and AuNPs are connected only to form clusters. The ratio N_{BS}/N_{AuNP} determine the number of BS on a single AuNP, which is two times that of Case I. The schematic illustration is given in Fig. 1A (i).

Case II. Nonetheless, in most cases the eq. S1 can be simplified as intermediate condition, where $0 < \boldsymbol{I} < 1$ is satisfied. Some BS molecules are connected by two AuNPs but some others are just cover the surface of AuNPs,

$$\boldsymbol{A} \times \boldsymbol{P} = (2-\boldsymbol{I}) \times N_{BS}/N_{AuNP} \qquad [0 \le \boldsymbol{P} \le 1,\ 0 < \boldsymbol{I} < 1] \tag{S4}$$

Therefore, the degree of inter-linking is expressed as a function of N_{BS}/N_{AuNP}.

Number of cluster, $N_{cluster}$. The total number of BS-linked AuNP clusters, $\boldsymbol{N}_{cluster}$ is defined as

$$N_{cluster} = \boldsymbol{I} \times N_{AuNP} + (1 - \boldsymbol{I}) \qquad [\boldsymbol{I} = 0 \text{ or } \boldsymbol{I} = 1] \tag{S5}$$

The boundary conditions for the above relation

: $\boldsymbol{I} = 1$ (thus $\boldsymbol{B} = 1$), $N_{cluster} = N_{AuNP}$

: $\boldsymbol{I} = 0$ (thus $\boldsymbol{B} = 2$), $N_{cluster} = 1$

However, for most cases where the condition, $0 < \boldsymbol{I} < 1$ is satisfied, the relation is a function of the number of AuNPs.

$$N_{cluster} = \boldsymbol{I} \times N_{AuNP} + (1 - \boldsymbol{I}) \qquad [0 < \boldsymbol{I} < 1]$$

For a given N_{AuNP} , the total number of reaction sites becomes ($N_{AuNP} \times \boldsymbol{A} \times \boldsymbol{P}$). Among those active sites, the bi-active BS, $(1 - \boldsymbol{I})\ N_{BS}$ choose 2 points from each non-identical AuNPs for linkage formation. However, the reactivity of the active sites on a single AuNP is not supposed to be differentiated for BS anchoring (such as geometrical torsion is not considered), thus ($\boldsymbol{A} \times \boldsymbol{P}$)! is divided.

$$\frac{(N_{AuNP}\,\boldsymbol{AP})C_{2}(\boldsymbol{AP})}{(\boldsymbol{A}\,\boldsymbol{P})!} = \frac{(N_{AuNP}\,\boldsymbol{A}\,\boldsymbol{P})P_{2}(\boldsymbol{A}\,\boldsymbol{P})}{2(\boldsymbol{AP})!\ (\boldsymbol{AP})!} = \frac{(N_{AuNP}\,\boldsymbol{AP})!}{2(\boldsymbol{AP})!\ (\boldsymbol{AP})![(N_{AuNP}-2)\times \boldsymbol{AP}} \tag{S6}$$

Therefore, from the above relation, the # of cluster, $N_{cluster}$ is proportional to N_{AuNP} and inversely proportional to $\boldsymbol{AP}$,

$$N_{cluster} \propto N_{AuNP}/\boldsymbol{AP} \qquad [0 < \boldsymbol{I} < 1] \tag{S7}$$

Network formation. There is a trade-off between the network formation and the surface covering by BS molecules, because the added BS can interlink AuNPs and simultaneously coat the surface of a AuNP. Suppose that the single AuNP is placed on a site of a lattice (Scheme S1, I) and added BS contribute to the interlinking between the AuNPs (Scheme S1, II), leading to branched polymer structure formation. By the Kramers theorem, the mean-square radius

of gyration (R_g) of an ideal molecule that contains randomly branched ***n***-mer and ***n*** freely jointed segments of length *b* but no loop, becomes (47–48)

$$<R_g^2> \cong b^2 \boldsymbol{n}^{1/2} \sqrt{\pi(f-1)/8(f-2)} \tag{S8}$$

f is the dimensionless functionality. The above relation is extended into two kinds of molecules by considering that the R_g of an ideal randomly-branched polymer is much smaller than that of an ideal linear chain having the same number of monomers. The dependency of the degree of polymerization for randomly-branched polymers becomes

$$R_g \approx b\boldsymbol{n}^{1/4} \tag{S9}$$

Meanwhile, for an ideal linear polymer, the relation

$$R_g \approx b\boldsymbol{n}^{1/2} \tag{S10}$$

is satisfied.

In general, using randomly-branched polymer model, the correlation length ζ for percolation is the size of the characteristic branched polymer with ***n*** monomers. Randomly-branched polymers are fractals, so the size ***R*** and the number of monomers ***n*** in a polymer are related by the fractal dimension ***D***,

$$\boldsymbol{n} \sim \boldsymbol{R}^{\boldsymbol{D}} \tag{S11}$$

The same relation is valid for the characteristic branched polymer,

$$\boldsymbol{n}^* \sim \boldsymbol{\zeta}^{\boldsymbol{D}} \tag{S12}$$

Since $\boldsymbol{n}^*$ diverges at the gel point with exponent 1/σ, the correlation length is also diverged,

$$\boldsymbol{\zeta} \sim (\boldsymbol{n}^*)^{1/\boldsymbol{D}} \sim |\varepsilon|^{-\nu} \tag{S13}$$

The exponent ν describing the divergence of the correlation length is related to σ and the fractal dimension ***D*** by the relation,

$$\nu \sim \boldsymbol{1/D}\sigma \tag{S14}$$

In the mean field, σ = 0.5, ***D*** = 4, so ν = 0.5 is satisfied. For the three-dimensional percolation, this critical exponent becomes ν = 0.88, thus the fractal dimension of randomly branched polymers in the polymerization reactor is ***D*** = 2.53 (38).

For critical percolation, the exponent ν and the fractal dimension $\boldsymbol{D}$ are related to the critical exponent by the hyper-scaling. Under the hyper-scaling condition, polymers with a given number of monomer, $\boldsymbol{n}$, are overlapped because they have many contacts and have already reacted to make a large polymer. The pervaded volume for a randomly-branched polymer with $\boldsymbol{n}$ monomers in $\boldsymbol{d}$-dimensional space is proportional to the relation by utilizing dimensionless space dimension (for a gel $1 < \boldsymbol{d} < 6$),

$$\boldsymbol{R}^{\boldsymbol{d}} \sim \boldsymbol{n}^{(\boldsymbol{d}/\boldsymbol{D})} \tag{S15}$$

Transmission electron microscopy (TEM) results of the clusters. Fig. S1 represents two types of AuNP assemblies. Fig. S1A shows the representative chemically-linked AuNPs by BS molecules suggested in this study (the selected condition of N_{BS}/N_{AuNP} = 2 (Cluster I) and 1 (Cluster II), respectively). Even though AuNPs are assembled, the individual AuNP can be identified with overlapped shadows. On the other hand, Fig. S1B displays the AuNPs treated by the ultrasonicater for more than an hour, by this procedure the AuNPs are expected to be fused into each other. The assemblies seem to be one large chunk where there is no local darkness difference. The designed clusters in this study exhibit individual AuNP, which are differentiated from the fused AuNPs.

Electron beam (e-beam). Scheme S2 summarizes the facility of the Pohang Neutron Facility (PNF). It consists of an electron linac, a water-cooled Ta target, and an 11m long time-of-flight (TOF) path. The electron linac consists of a thermionic RF-gun, an alpha magnet, four quadrupole magnets, two SLAC-type accelerating sections, a quadrupole triplet, and a beam-analyzing magnet. A 2-m long drift space is added between the first and the second accelerating section to insert an energy-compensation magnet or a beam-transport magnet. The overall length of the linac is about 15 m. The RF-gun has one cell cavity with a dispenser cathode of 6 mm in diameter. The RF-gun produces electron beams of 1 MeV, 300 mA, and 1.5 ms. Four quadrupole magnets are used to focus the electron beam in the beam transport line from the thermionic RF-gun to the first accelerating section. The quadrupole triplet installed between the first and the second accelerating sections is used to focus the electron beam during the transport to the experimental beam line at the end of the linac. The available RF power from a SLAC 5045 klystron is 45MW at the maximum due to the peak power limitation of the pulse modulator. The RF power fed to the RF-gun is 3MW. The beam energy is 80 MeV. The measured beam currents at the entrance of the first accelerating section and at the end of the linac are 100 and 40 mA, respectively. The width of an electron beam is 3 μs pulse, and the pulse repetition rate is 10 Hz. The electron beam is about 20 mm in diameter at the beam profile monitor in front of the target. The measured energy spread is less than 1 %. The e-beam is directly applied to the designed AuNP

solutions in Whirl-Pak® sample bag (B00679WA model, Nasco, USA) for the duration times of 5 and 15 min. Due to known resistance at the Ta target (2 Ω), the total electrons reaching to the samples can be calculated in relative scales by the voltage vs. time data shown in Fig. S2. For all the samples, the amount of electrons is confirmed to be similar without significant deviations.

fs-THz spectroscopy. The fs-THz beamline at the Pohang Accelerator Laboratory (PAL) supplies ultrafast and intense THz radiation from a 75 MeV linear accelerator as well as the Ti:Sapphire laser amplifier system (49). For this research a Ti:Sapphire laser amplifier system (Coherent Inc.) was used for the terahertz time domain spectroscopy. The output pulse energy was 3 mJ at the repetition rate 1 kHz. When properly compressed, duration of the amplified pulses was 120 fs. About 1 mJ of the 800 nm pulses out of the regenerative amplifier was split into two by a beam splitter. One part (up to 350 μJ) was delivered onto a THz emitter, a 10x10 mm <110> ZnTe crystal with a thickness of 1 mm, to generate femtosecond THz pulses via optical rectification. The emitted THz radiation was focused and collimated by two off-axis parabolic mirrors. The THz radiation is detected by electro-optic sampling method using another 1 (or 0.5) mm thick ⟨110⟩ ZnTe nonlinear crystal. The remaining energy from the 800 nm pulses with pulse energy of 50 μJ is temporally delayed using an optical delay line and then focused by a lens collinear with the THz beam onto the ⟨110⟩ ZnTe crystal. The THz field induces birefringence in the crystal and the polarization of the probe pulse is rotated in proportion to the THz field. It can be measured by a combination of a quarter-wave plate, a Wollaston polarizer, and a pair of balanced photodiodes. The signal current is sent to a lock-in amplifier (Stanford Research System, SR830). A silicon window of high resistivity and a THz low-pass filter (Microtech, Inc.) are used to remove the residual pump beam. Specially designed quartz crystal is used as the windows of the sample holders to maximize the fs-THz transparency.

References

47. R. Kopelman. *Science* **241**, 1620 (1988).

48. D. W. Schaefer. *Science* **243**, 1023 (1989).

49. J. Park. *et al. Rev. Sci. Instrum.* **82**, 013305 (2011).

Table S1. AuNP stock solution (1×10^{-9} mmole AuNP/mL), BS stock solution (1×10^{-4} mmole BS/mL), 0.1, 1, 1.5, 2, 3 and 4 mL are added to 100 mL AuNP stock solution. N_{AuNP}: total # of AuNPs, N_{BS}: total # of Bismuthiol.

	N_{BS} ($\times 10^{-4}$ mmole)	N_{AuNP} ($\times 10^{-7}$ mmole)	N_{BS}/N_{AuNP} ($\times 10^{3}$)
BS 0	0	1	0
BS 0.1	0.1	1	0.1
BS 0.3	0.3	1	0.3
BS 0.5	0.5	1	0.5
BS 1	1	1	1
BS 1.2	1.2	1	1.2
BS 1.5	1.5	1	1.5
BS 1.8	1.8	1	1.8
BS 2	2	1	2
BS 2.5	2.5	1	2.5
BS 3	3	1	3
BS 4	4	1	4

Scheme S1. Lattice model for the AuNP interlinking by BS molecules. AuNPs are placed on a lattice (I) and BS molecules interlink the AuNPs (II).

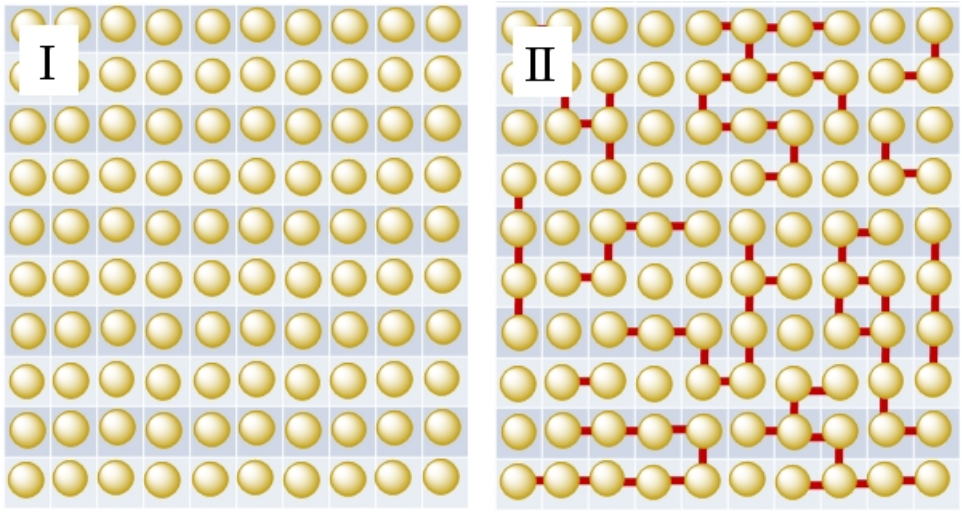

Scheme S2. e-beam facility and experimental set-up

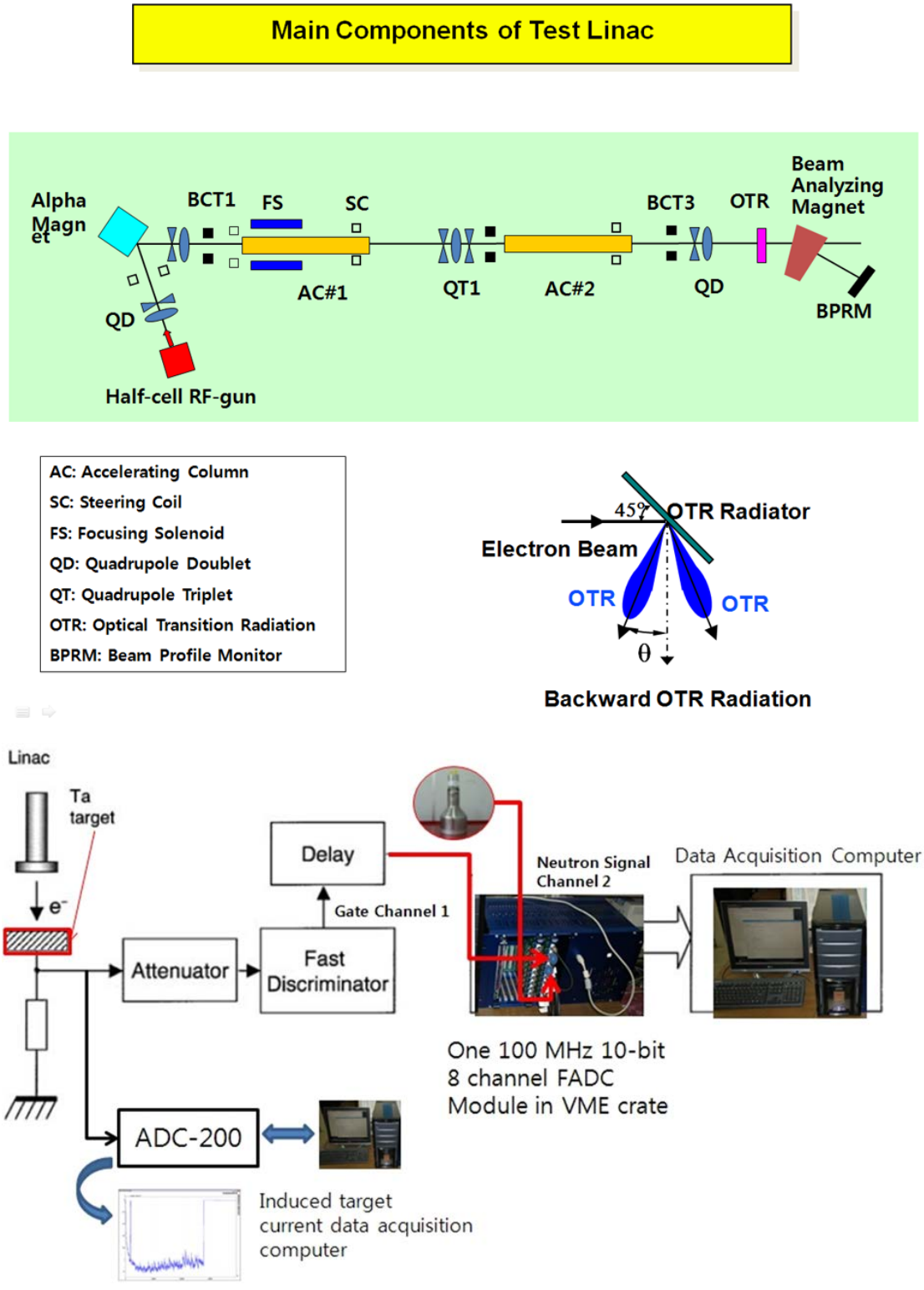

Figure S1. Transmission electron microscopy (TEM) results of the chemically-linked clusters (Cluster, **A**) and chemically fused aggregate (Chemical aggregate, **B**) AuNPs.

A.

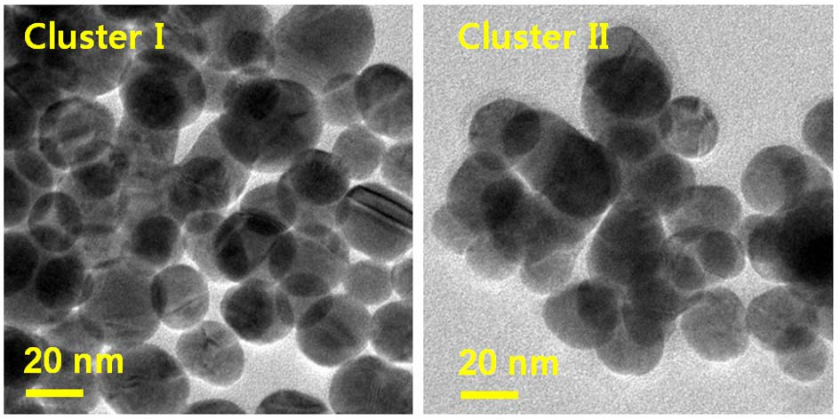

B.

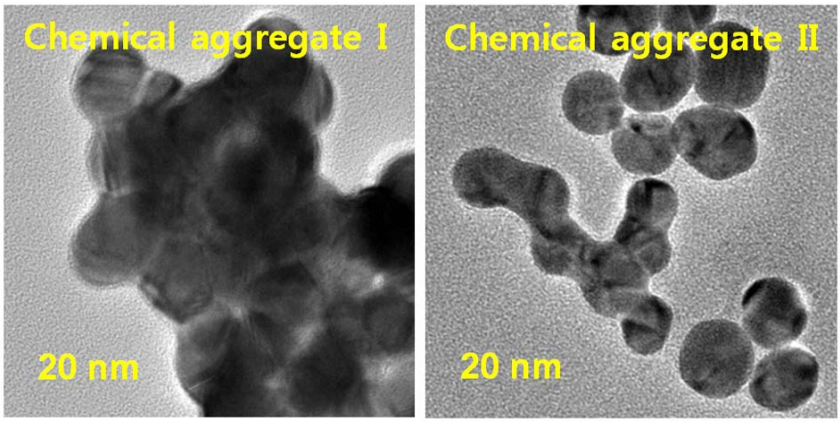

Figure S2. Electron beam treatment of each sample investigated in this study. With a fixed resistance (Ω) at the measurement point, the voltage (V) change for given time duration can be converted to total electron flow. Voltage vs. Δ time for **(A)** 5min and **(B)** 15 min exposure to e-beam.

A.

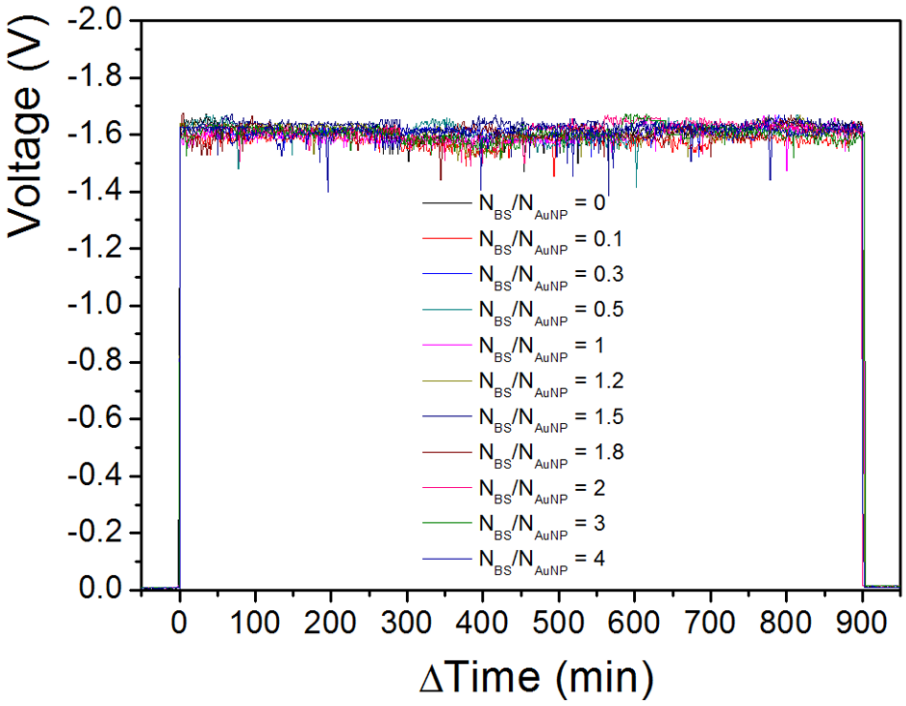

B.